ELSEVIER

Polymer 40 (1999) 7261–7274

polymer

The breaking strength of ultra-high molecular weight polyethylene fibers

J. Wang, K.J. Smith Jr.*

Department of Chemistry, College of Environmental Science and Forestry, State University of New York, Syracuse, NY 13210, USA

Received 7 January 1997; received in revised form 19 December 1998; accepted 6 January 1999

Abstract

Ultimate mechanical properties of polyethylene fibers were measured. Results are in close agreement with the stress-induced melting theory of fracture (for finite molecular weight polymers). The perfect fiber work of rupture W_c, modulus K_c, strength σ_c, and strain ε_c are found to be $W_c = 0.084 \pm 0.003$ GPa; $\sigma_c = 7.5$ GPa; $K_c = 335 \pm 12$ GPa; $\varepsilon_c = 0.0225 \pm 0.0005$. The activation energy of fracture is measured as ≈ 108 kJ/mol—the activation energy of polyethylene fusion and one-third the activation energy of bond scission. Non-uniformity of fibers necessitates averaging properties over several test lengths. Actual stress-strain curves are decomposed into thermodynamic and irreversible components. Fusion theory applies to the thermodynamic component.. © 1999 Elsevier Science Ltd. All rights reserved.

Keywords: Ultra-high molecular weight polyethylene; Fusion theory

1. Introduction

Gel spun fibers of ultra-high molecular weight polyethylene (UHMWPE)—at least 3×10^6 kg/kmol—now are routinely processed into high strength, high modulus fibers via the technique primarily developed by Smith and Lemstra [1–6] and Pennings [7–12], with various co-workers. Processed fibers exhibit tensile strengths and moduli upwards to about 7 GPa and 230 GPa, respectively. Somewhat higher results are occasionally reported for individual fibers, but these appear to be spurious. In fact, in this study we observe apparent individual fiber strengths as high as 10.5 and 11.3 GPa, certainly unreliable figures generated by large happenstance inherent to fracture studies that are not properly averaged.

Anticipation of super-strength fibers has been the primary motivation behind many, perhaps most, studies of polymeric fibers in recent decades. Invariably, covalent bond scission has been accepted, with little or no caution and reflection, as the determinate of strength. The train of thought begins with diamond, a material of exceptionally high strength attributed to its tetrahedral lattice structure of covalently bonded carbon atoms—i.e. a covalently bonded crystal. Fracture of the crystal must of necessity proceed only via bond scission. Ergo, a linear polymer, composed of long chains of covalently bonded repeating units, must have strength along the polymer backbone determined by the covalent bond strength of its constituent atoms. As covalent bonds are of high strength, all one need do to prepare very high strength fibers is extend and align the polymer molecules so as to form an oriented crystalline fibrous structure. The fiber then fails whenever a tensile force is sufficient to rupture the necessary molecular bonds of the unidimensional covalently bonded fibrous crystal.

The strength of such a bond, at least one of those in polyethylene, was calculated [13] to be about 19 GPa, which implies a similar figure, more or less, for a fully formed, perfect polyethylene fiber. Also Zhurkov et al. [14–17] claimed experimental support for molecular bond scission as the mechanism of polymer fiber fracture. His approach is *kinetic* in origin, based on the time required for fiber rupture under a constant load.

Thus the bond scission mechanism of fracture, but it is not correct for polymers of finite molecular weight. First, polyethylene fibers with moduli quite close to the expected maximum do not break at the expected 19 GPa range but rather at 6–7 GPa, with little hope for significant increase. Second, Zhurkov's kinetic interpretation is problematical [18] and is wrong outright for polyethylene based on data reported herein and the arguments in Ref. [18]. The Zhurkov interpretation requires an activation energy of bond scission, which is ~80 kcal/mol for a carbon–carbon bond, but our measurements give only 26 kcal/mol for what should be the anticipated value. This large discrepancy by a factor of 3

* Corresponding author. Tel.: + 1-315-470-6854; fax: + 1-315-470-6856.

0032-3861/99/$ - see front matter © 1999 Elsevier Science Ltd. All rights reserved.
PII: S0032-3861(99)00034-8

poses very serious problems for the scission theory that are unlikely to be rationalized away in a convincing fashion. Actually, the experimental value of 26 kcal/mol appears to be the activation energy of fiber fracture via a mechanism of stress-induced melting [18,19], which is posited on thermodynamics rather than kinetics, although some considerations of kinetic influences are required. Third, the consequences of polymer molecular weight have been overlooked in fracture theory, obliterating a critical distinction between finite and infinite (effectively) molecular weight—to wit, a fibrous crystal stabilized by intermolecular forces (i.e. normal crystalline forces) or a crystal of unbroken covalent bonds along the fiber axis, clamp to clamp. The latter requires bond scission for fiber failure where the former does not, only an overriding of van der Waals crystalline forces. So long as polymer contour length is insufficient to span unbroken the complete fiber length, the weaker van der Waals forces must determine the tensile strength. A tensile force therefore destabilizes such bonds and lowers the fiber (crystalline) melting temperature. A force great enough to depress the melting point to ambient temperature causes melting and fiber failure. This situation has been treated thermodynamically [19], yielding ~7–8 GPa for perfectly formed fibers of finite molecular weight polyethylene, which is exactly the range of the best experimental values. Thus, no serious discrepancy between experimental and theoretical strengths of polyethylene fibers in fact exists according to the thermodynamic fusion theory. In contrast, if molecular weight is great enough to span the entire length of the macroscopic fiber, clamp to clamp, fusion cannot be induced by tension; in fact, tensile stress should further stabilize the crystal structure. Failure might occur in this case by bond scission, probably at about 19 GPa stress [13]. However, such high molecular weight polymers are not now available.

In this article we report the results of our general study of the breaking strength of UHMWPE fibers, the aim of which is to estimate the ultimate strength and modulus of the perfect fiber and to assess the validity of the thermodynamic fusion theory of fiber strength of perfect and imperfect fibers [18,19].

2. Experimental details

GUR 412 (Hostalen GUR UHMW Polymer) was kindly provided by Hoechst Celanese Cooperation, Houston, Texas. Its weight-average molecular weight is $\sim 5 \times 10^6$ kg/kmol and its disperse index is 5–7 (i.e. its number-average molecular weight is $6–7 \times 10^5$ kg/kmol), according to the report from the factory. However, M. Matsuo et al. reported that GUR 412's molecular weight distribution index is 12–20. (i.e. its number-average molecular weight is only $4–2.5 \times 10^5$ kg/kmol.) This raw material was only used in some preliminary selected experiments.

Himont 1900 UHMWPE is the primary material used in this study. It was kindly provided by Himont USA, Inc., Lake Charles, LA, USA. Its weight-average molecular weight is 5.5×10^6 kg/kmol and the number-average molecular weight is 2.5×10^6 kg/kmol. Its disperse index is as low as 2.2.

Decalin (Decahydronaphthalene, $C_{10}H_{18}$), produced by Sigma Chemical Co., is the polymer solvent. Its boiling point is ~188°C.

2.6-Di-tert-butyl-4-methylphenol (2.6-ditertiary-butyl-*p*-cresol or DBPC) is the anti-oxidant. Its chemical formula is $[(CH3)3C]_2\ C_6H_2\ (CH_3)$ OH. It is produced by Pfaltz & Bauer, Inc., a Division of Aceto Corporation.

2.1. UHMWPE gel-solution preparation

The UHMWPE gel-solutions were prepared by mixing Himont 1900 UHMWPE powder (1.5% w/w in the initial concentration) with solvent Decalin (98% w/w in the initial concentration) and anti-oxidant 2,6-Di-tert,-butyl-4-methylphenol (0.5% w/w in the initial concentration) in a 100 ml round-bottom flask with three-necks and heated in an oil bath up to 130°C. Nitrogen N_2 was used to prevent oxidative degradation. Gentle stirring was continuous throughout. When the temperature reaches ~105°C, the UHMWPE powder begin to dissolve. Further heating to 130°C completes the solution. This temperature is maintained at least for 30 min. A uniform UHMWPE gel-solution is obtained in this fashion.

2.2. Fiber spinning apparatus and procedures

The major units of the fiber spinning apparatus are an extrusion compartment and a coagulation bath. For UHMWPE, the coagulation bath is air at room temperature. The extrusion compartment consists of a stainless-steel syringe, a driving screw with a reversible, synchronous, permanent magnet motor, and a set of automatic switches to control the motor. The hole diameter of the spinneret is 0.5 mm and its thickness is 3 mm. The outside of the extrusion syringe is covered by a heating bandage to maintain a constant syringe temperature of 130°C. Before and after introducing UHMWPE gel-solution, the syringe is flushed with N_2 to prevent gel oxidation. After inserting the piston, and before spinning, the syringe is kept at constant temperature 130°C for 30 min to insure uniform temperature. Then, the gel solution is extruded and coagulated in air to yield original fibers. Subsequently, these fibers are dried in air for 48 h to evaporate the solvent decalin, then vacuum dried for another 24 h.

2.3. Hot-drawing apparatus and procedures

The original fiber has a low breaking strength due to its very low degree of orientation. Hot-drawing is necessary to raise the ultimate strength and modulus of the fiber. The hot-drawing apparatus is composed of three parts: a tube oven, a pre-heating coil, and a circulating oil bath. The tube oven is

a copper pipe 65 cm long and 35 mm in diameter, which is covered by a heating bandage. A variac controls the temperature of the tube oven (usually 125°C). The circulating oil bath is used as a hot oil reservoir for the pre-heating coil. The oil bath temperature is usually maintained at 125°C, almost the same as that of the tube oven. Nitrogen N_2 is pre-heated in a coil, which is a small copper tube of 2 m length and 5 mm diameter immersed in the oil bath inside a large copper cylinder of 32 cm long and 55 mm in diameter horizontally set under the tube oven. The pre-heated N_2 is blown into the tube oven to provide a necessary hot-atmosphere for hot-drawing and to prevent fiber oxidation.

After the hot-drawing system reaches a stable temperature (usually 125°C), a known length (measured before hot-drawing) of dried original UHMWPE fiber is introduced into the tube oven. The original fiber is held there for around 1 min before drawing; then, the hot-drawing is begun by turning a winding wheel. After high drawing, a very fine UHMWPE super strong fiber is obtained. The total length of the drawn fiber is measured so that the draw ratio can be determined.

2.4. Characterizations of fibers

Most characterization methods relate to tensile properties. In addition, we also use DSC, SEM, and X-ray to characterize crystallinity and morphology of UHMWPE super fibers.

2.5. Determination of cross-section area of fibers

The fiber cross-section area, A, is determined by weighing a known length L of fiber. From the density and length the average cross-sectional area can be calculated. As strength measurements, etc., are generally not of very high precision, a common practice in the literature [20] is to use the crystalline density of 1 g/cm^3 at 25°C for all fibers. This is the value we used. Likely error is probably around 2%. Therefore this yields the *average* cross-section area along the entire fiber length. All test lengths cut from the fiber must therefore be averaged over breaking forces and divided by average area to obtain the average stress over several test lengths of a single long fiber.

2.6. Tensile test of fiber's breaking strength

The ultimate mechanical properties of the UHMWPE fibers were determined by an Instron Tensile Tester. The original test length was set at 25 mm, which is the initial distance between the two clamps. Hollow PE fibers were used to protect the fiber from clamp damage during testing. The rate of fiber deformation is $6.67 \times 10^{-3}\,s^{-1}$ (i.e. the crosshead of the tensile tester moves down at the rate of 1 cm/min.) All tests were done at room temperature.

2.7. Differential scanning calorimetry

Differential Scanning Calorimetry (DSC) studies were performed on a Perkin-Elmer DSC-4 scanning calorimeter, which was purged with nitrogen gas to provide an inert atmosphere during testing. The amount of sample was ca. 10 mg. The temperature scale of the calorimeter was calibrated with an indium standard reference ($T_m = 156.60$°C). The scanning range was usually 50–180°C for UHMWPE samples.

2.8. Wide angle X-ray diffraction (WAXD) analysis [21,22]

X-ray was used to measure the crystallinity of UHMWPE fibers. The instrument is a Rigaku X-ray diffractometer operated at 50 kV voltage and 140 mA current.

The range of the X-ray scanning angle 2θ is usually 15–30° for crystallinity determination because the crystal peaks are located ca. 22 and 24.5° for UHMWPE. The sample tested was a group of tiny UHMWPE fibers (usually 5–8 pieces depending on the size of fibers). To get the greatest diffraction intensity, the sample was rotated from 0 to 360° (i.e. β direction 0–360° scanning) to locate the best orientation angle (usually 0–5°). Owing to the small amount of sample required for X-ray analysis, the crystallinity of each individual fiber can be determined.

2.9. Scanning electron microscopy

To investigate the non-uniformity of fiber cross-section, scanning electron microscopy (SEM) was used. Fibers were coated with gold/platinum for secondary image analysis. The total coating time of 2.5 min was divided into 5 s intervals between which a 60 s cooling time was applied to reduce the temperature in the vacuum chamber of the sputter coater in order to avoid possible damage of the delicate fiber samples when the gold/platinum was coated onto the samples. The SEM experiments were performed by an ETEC autoscanning electron microscope operated at voltage 20 kV, high vacuum less than 1×10^{-4} Torr, and condenser spot size 2.4–2.5 A. The photographing secondary electron image was set at contrast 2.80, brightness 4.00, and lens opening F-16 for Polaroid film.

3. Results and discussion

Effects of molecular weight and molecular weight distribution on the breaking strength of UHMWPE fibers: The mechanical strength of polyethylene fibers increases rapidly as the molecular weight of the polymer increases up to a certain molecular weight limit. Above that molecular weight, strength tends to a constant value. Prevorsek [23] points out that $M_n = 60\,000$ is sufficient to achieve a strength exceeding 95% of the theoretical maximum at infinite molecular weight. Molecular weight distribution,

Table 1
Ultimate properties of GUR 412 and Himont 1900 fibers

GUR 412			Himont 1900		
σ_* (GPa)	ε_*	K_i	σ_* (GPa)	ε_*	K_i
1.30	0.037	32.3	2.62	0.082	49.7
1.42	0.041	47.2	3.20	0.068	70.8
1.42	0.053	50.8	3.68	0.071	65.8
1.64	0.063	31.7	4.38	0.076	81.3
2.00	0.042	65.4	4.67	0.052	142.0
2.11	0.051	51.4	5.12	0.039	146.0
2.16	0.061	50.0	5.60	0.058	137.0
2.33	0.041	86.3	5.89	0.048	196.0
2.76	0.046	76.0	6.04	0.052	180.0
3.09	0.047	108.0	6.38	0.034	214.0
3.11	0.047	91.6	6.83	0.060	195.0
3.63	0.054	99.0	7.15	0.034	246.0

however, seems an important factor affecting the mechanical properties of materials [24].

We used two kinds of UHMWPE, GUR 412 and Himont 1900, as raw materials to make UHMWPE fibers. Our tensile results show that Himont 1900 fibers are stronger than GUR 412 fibers (see Table 1). Fiber preparation procedures for both were identical, and the weight-average molecular weights (5×10^6 for GUR 412 and 5.5×10^6 for Himont 1900) are almost identical. GUR 412 gave a maximum fiber strength around 4 GPa (most were around 2 or 3 GPa). However, Himont 1900 produced two fibers of over 7 GPa and many over 4 GPa. This is because of their different molecular weight distributions. The disperse index of GUR 412 is 7, and that of Himont 1900 is 2.2. Thus, the number average molecular weight of the former is only 7×10^5, but that of the latter is 2.5×10^6. It is obvious there are many more short polymer molecules in GUR 412 than in Himont 1900. These short molecules probably increase the number of defects in the fiber, which are the weakest points, and which determine the fiber strength (imperfect fibers). We expect, therefore, GUR 412 fibers to be much weaker than Himont 1900 fibers. Accordingly, both molecular weight and molecular weight distribution play important roles in determining the mechanical properties of polymers.

Creep behavior of GUR 412 fibers: A few fibers of GUR 412 were used to determine the time required for a constant, suspended load (creep) to break the fibers. The fibers were prepared as described herein but the results are reported and discussed in the preceding article [18]. No further comment here on these results except to point out that the experimental temperature was ~298°K.

Ultimate properties of UHMWPE fibers (Himont 1900): To study the mechanical properties of UHMWPE fibers, we prepared some high strength Himont 1900 UHMWPE fibers according to the procedures described herein. Ultimate mechanical properties were measured with an Instron. The results are shown in Table 2. The first column gives the number of test lengths cut from a single long fiber (50–100 cm) and tested with the Instron. Each fiber entry in

Table 2
Ultimate properties of UHMWPE fibers (Himont 1900)

Number of test lengths	$A \times 10^{10}$ (m^2)	λ	σ_* (GPa)	ε_*	K_i (GPa)
(4)	14.06	30	2.35	0.080	39.2
(5)	6.582	25	2.58	0.086	45.2
(4)	11.90	22	2.62	0.082	49.7
(4)	4.324	65	2.77	0.097	32.0
(4)	12.00	20	2.91	0.061	80.7
(5)	5.098	49	3.00	0.087	39.5
(5)	6.122	32	3.04	0.079	60.0
(4)	6.215	28	3.20	0.068	70.8
(5)	6.700	98	3.56	0.070	127
(4)	4.615	55	3.68	0.071	65.8
(4)	4.545	64	3.97	0.035	169
(4)	2.277	54	4.38	0.076	81.3
(4)	1.030	120	4.57	0.041	90.5
(5)	1.111	88	4.59	0.056	129
(5)	1.039	191	5.02	0.054	104
(5)	1.507	101	5.06	0.037	169
(4)	1.644	45	5.12	0.039	146
(4)	2.247	86	5.60	0.058	137
(5)	0.947	209	5.89	0.048	196
(4)	1.161	77	6.04	0.052	180
(4)	0.556	205	6.38	0.034	214
(4)	1.010	90	6.45	0.040	182
(4)	1.667	64	6.62	0.036	229
(5)	1.320	94	6.69	0.075	110
(4)	1.852	64	6.75	0.050	211
(5)	1.316	70	6.85	0.080	141
(5)	0.576	135	7.15	0.053	210

Table 3
Crystallinity and ultimate properties (Himont 1900)

Number of test lengths	$A \times 10^{10}$ (m^2)	λ	σ_* (GPa)	K_i (GPa)	ε_*	ω (%)
(4)	33.74	24	0.97	13.9	0.072	70.5
(4)	5.075	31	2.07	32.9	0.088	75.7
(4)	13.6	48	2.54	65.1	0.071	86.4
(5)	6.7	98	3.12	120	0.065	91.6
(5)	8.972	90	3.22	63	0.069	83.1
(5)	8.44	78	3.38	113	0.067	81.6
(4)	1.507	101	4.65	172	0.040	87.5
(5)	2.15	107	4.67	142	0.052	86.4
(5)	3.78	173	4.90	149	0.051	88.0
(4)	1.482	103	5.88	140	0.058	92.5
(4)	0.617	133	6.37	220	0.042	95.6
(5)	0.811	151	6.83	195	0.060	96.4
(4)	0.556	205	7.15	246	0.034	98.4

the table is an average value of the 4 or 5 short test lengths. The second column is the *average* cross-section area of each long fiber as determined by the weighing method. The third column is the draw ratio $\lambda = l/l_0$ or $\lambda = A_0/A$, where l_0 and A_0 are the length and the cross-section area of the undrawn fiber, and l and A are the length and the cross-section area of the drawn fiber. It is assumed that the volume V is unchanged when drawn.

The fourth column of Table 2 lists the average breaking strength, σ_*, and the fifth column gives ε_*, the average strain at break. The last column K_i is the average initial (Young's) modulus. All averages are over the 4 or 5 test lengths.

In Table 2 (and Table 3), it is seen that fibers of UHMWPE (Himont 1900) have superior tensile properties. The ultimate breaking strength is as high as 7 GPa, the

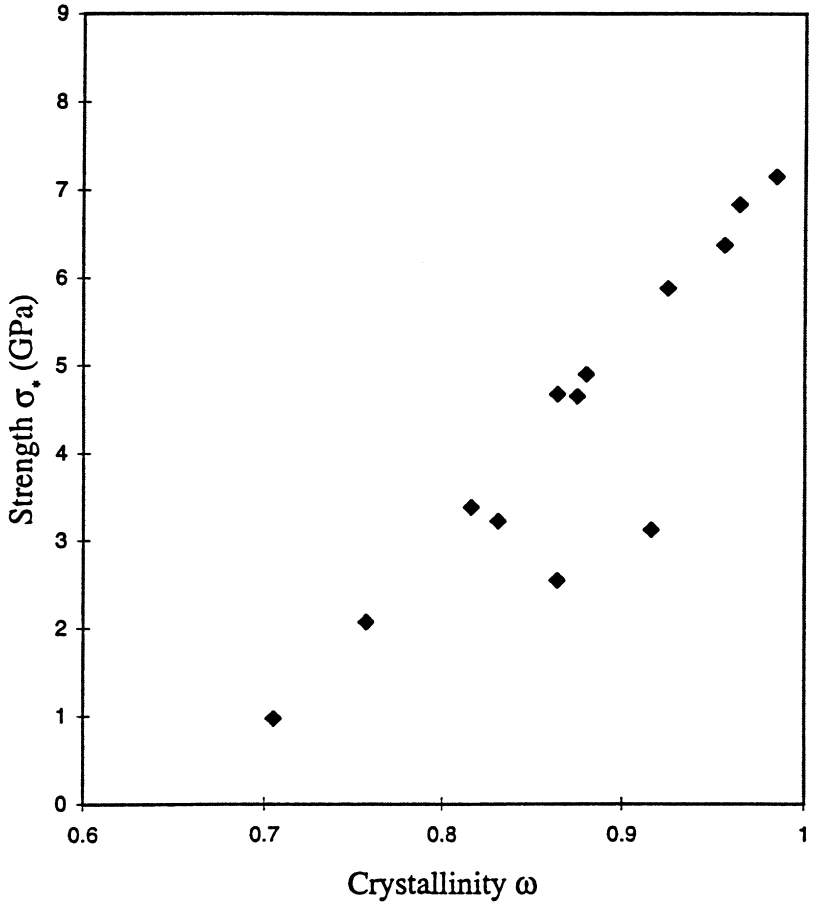

Fig. 1. Breaking strength vs. crystallinity.

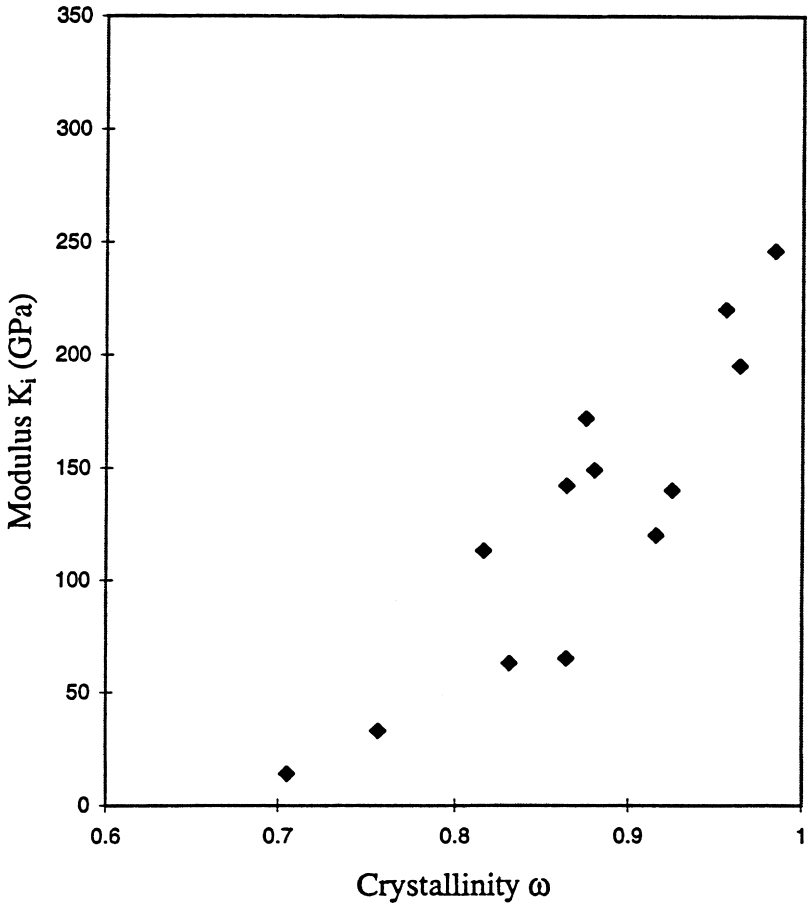

Fig. 2. Initial modulus K_i vs. crystallinity.

highest is 7.15 GPa. However, most fibers are located in the range of 4–6.5 GPa. Strains at break are generally small; the smallest one is 0.034 and most are around 0.050. In addition, the moduli are high, the highest is 246 GPa, very close to the crystalline modulus of 235 GPa measured by X-ray diffraction [25]. Such results are in line with the fusion theory, which gives the ultimate breaking strength of polyethylene as approximately 6.9 GPa if 235 GPa is the modulus of polyethylene. If the modulus is 300 GPa, or higher, the calculated theoretical strength is 7.8 GPa or higher [19]. Becasue a modulus of polyethylene of ~300 GPa is widely accepted, the experimental strength of 7.15 GPa is in good accord with the theoretical value of 7.8 GPa. Our experimental results do not conflict with the fusion theory since the theoretical value applies only to the ultimate strength of a *perfect* fiber, i.e. the maximum strength. *Real* fibers (less perfect) have strengths less than the maximum.

Dependence of ultimate mechanical properties on cross-section area and draw ratio: The data in Table 2 show that smaller cross-sections give greater breaking strengths. Very high breaking strengths occur if cross-section areas are close to or less than 10^{-10} m^2. If cross-section areas are greater than 10^{-9} m^2, the breaking strengths hardly reach 3 GPa. The Young's modulus K_i has a similar relationship with the fiber cross-section area although large scattering of data points occurs.

The strength increases as draw ratio increases, and the strain at break decreases. Young's modulus also increases with increasing draw ratio. However, these variations are less prominent once the draw ratio exceeds 50, which is consistent with Penning's results [20].

Crystallinity and ultimate properties: DSC was used to measure the melting points of batches of Himont 1900 powder, undrawn fiber, and drawn fiber. The results are 144, 139, and 147°C, respectively. Clearly, there is a small increase, ~3°C, from powder to drawn fiber. Further, we note that constraining fiber ends increases the melting temperature by 7 or 8° [26], which gives an effective melting point of our material, with ends fixed, of about 150–155°C. The fiber melting temperature, with constrained ends, is required in the fusion fracture theory.

To determine the variation of ultimate mechanical properties with crystallinity, thirteen long fibers were prepared, representing various draw ratios from low to high, and each was cut into four or five test lengths. The properties of each fiber were obtained by averaging the properties of its four or five test lengths, using for each the long fiber average cross-section area. The results are shown in Table 3. Crystallinities were determined via X-ray diffraction.

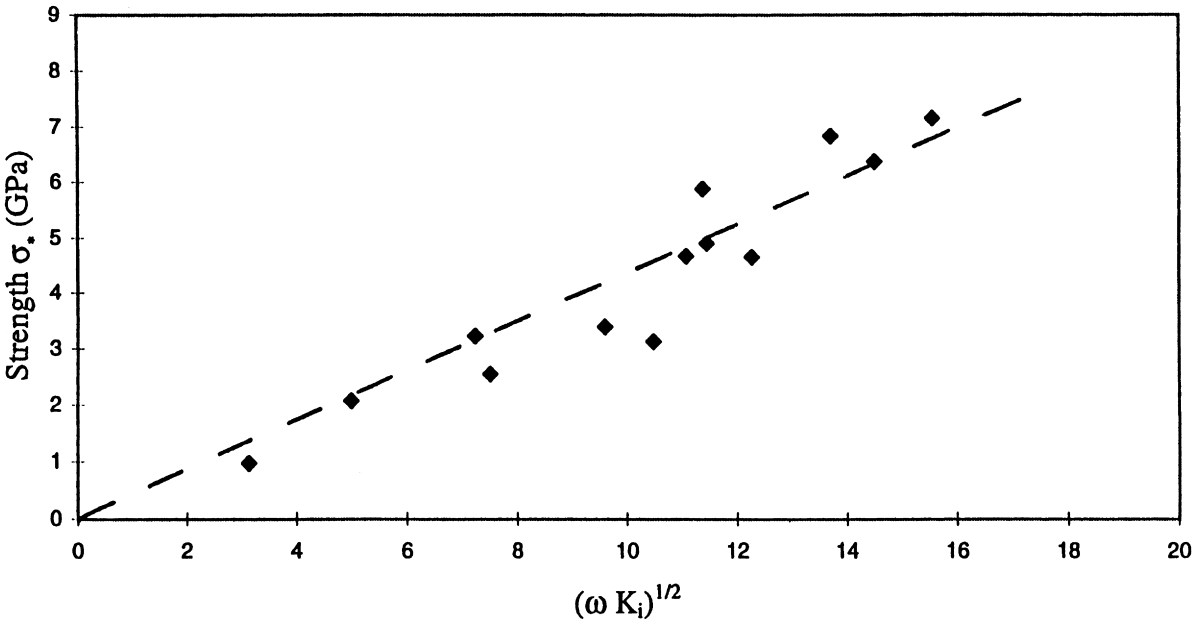

Fig. 3. Strength vs. $(\omega\ K_i)^{1/2}$.

Figs. 1 and 2 show the variations of breaking strength, σ_*, and initial (Young's) moduli, K_i, with fiber crystallinities, ω, in Table 3. The strength appears in Fig. 1 to be linear with crystallinity. As $\omega \rightarrow 1$, $\sigma_* \rightarrow \sigma_c$ extrapolates to ~7.3–7.7 GPa. However, at the lower levels of σ_* some curvature concave to the abscissa should exist, else fibers of crystallinities less than ~67% would be completely devoid of strength. Therefore, we should concede a strength for a perfect, completely crystalline fiber of about 7.5 GPa. The initial modulus, shown in Fig. 2, does not appear to be linear with ω. Therefore, it is nearly impossible to directly estimate with precision the value of $K_c = K_i(\omega = 1)$ of a perfect fiber ($\omega = 1$). It appears to lie between 275 and 350 GPa.

The fusion theory of fiber fracture in the preceding article [18] predicts strength to be

$$\sigma_* = [2\omega K_i W_c]^{1/2}, \tag{1}$$

where W_c is the work of rupture of the perfect fiber. Therefore, σ_* should vary linearly with $(\omega K_i)^{1/2}$. This is the case in Fig. 3. From the slope W_c is found to be 0.088 GPa.

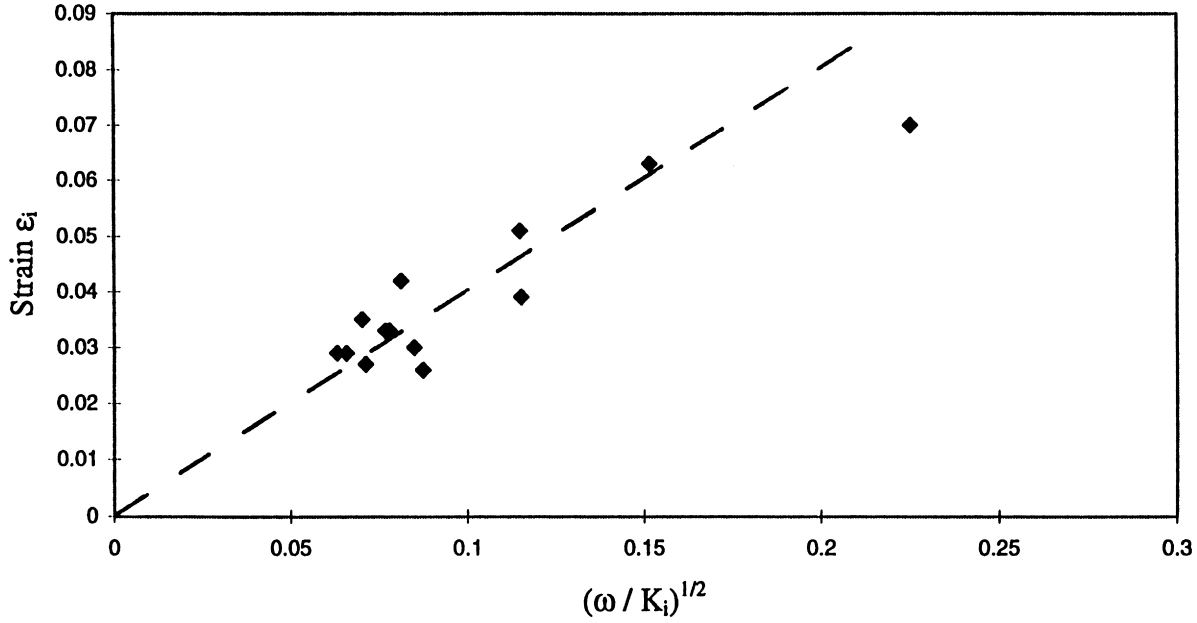

Fig. 4. Strain ε_i vs. $(\omega/K_i)^{1/2}$.

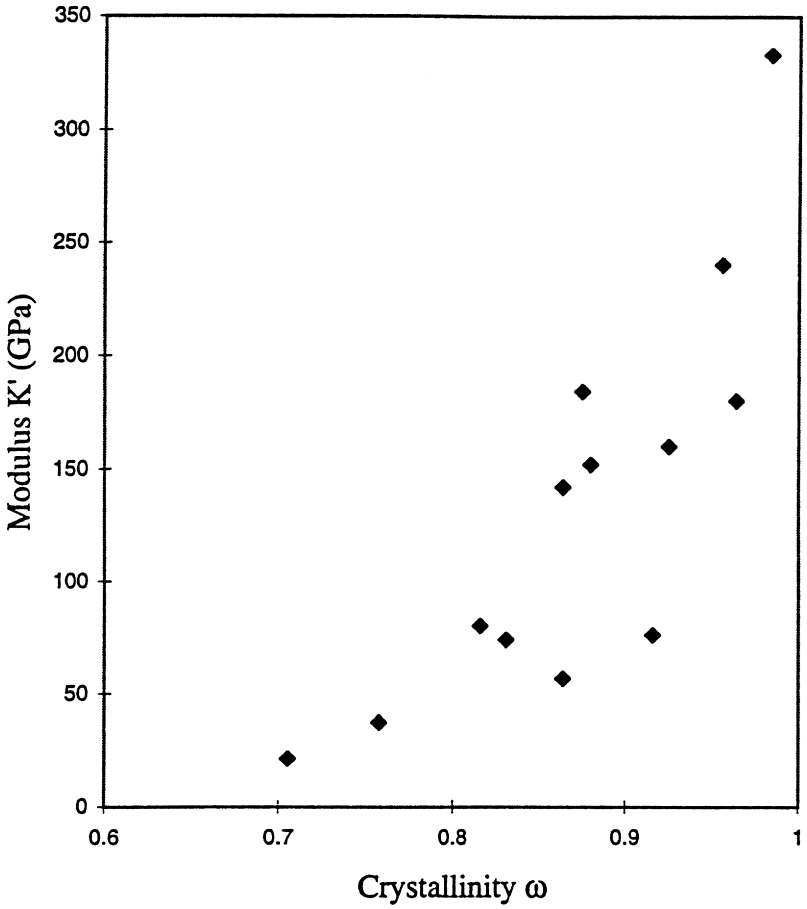

Fig. 5. Modulus K' vs. crystallinity.

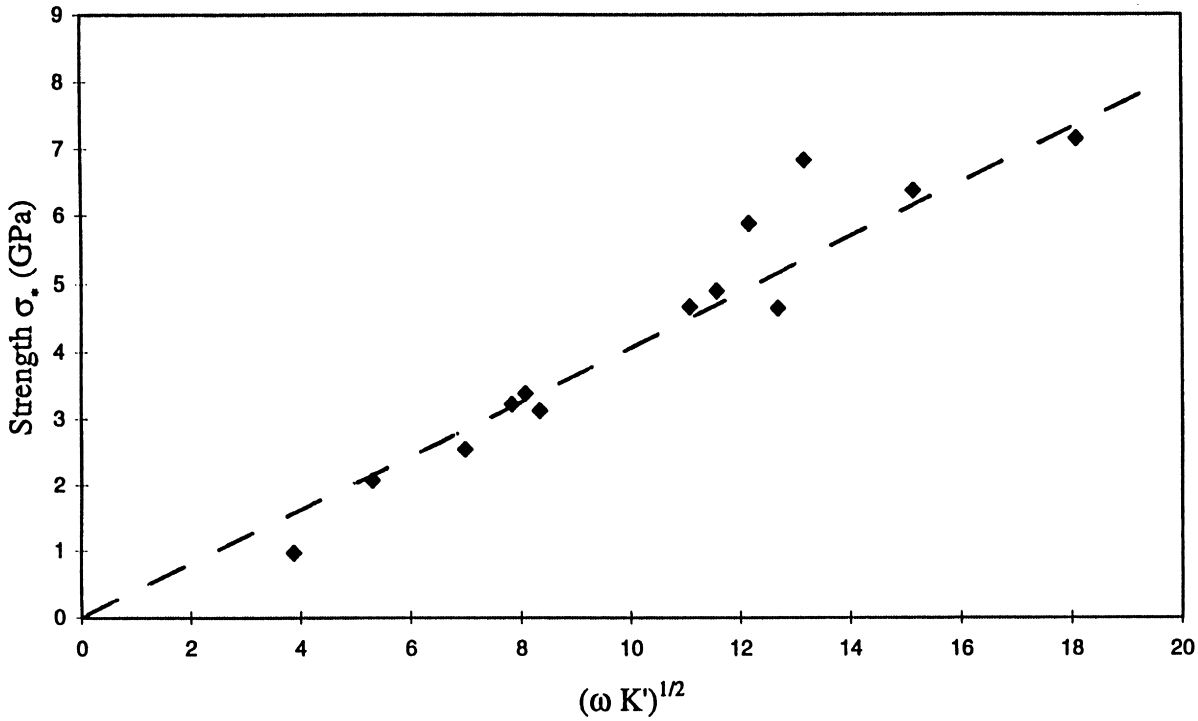

Fig. 6. Strength vs. $(\omega K')^{1/2}$.

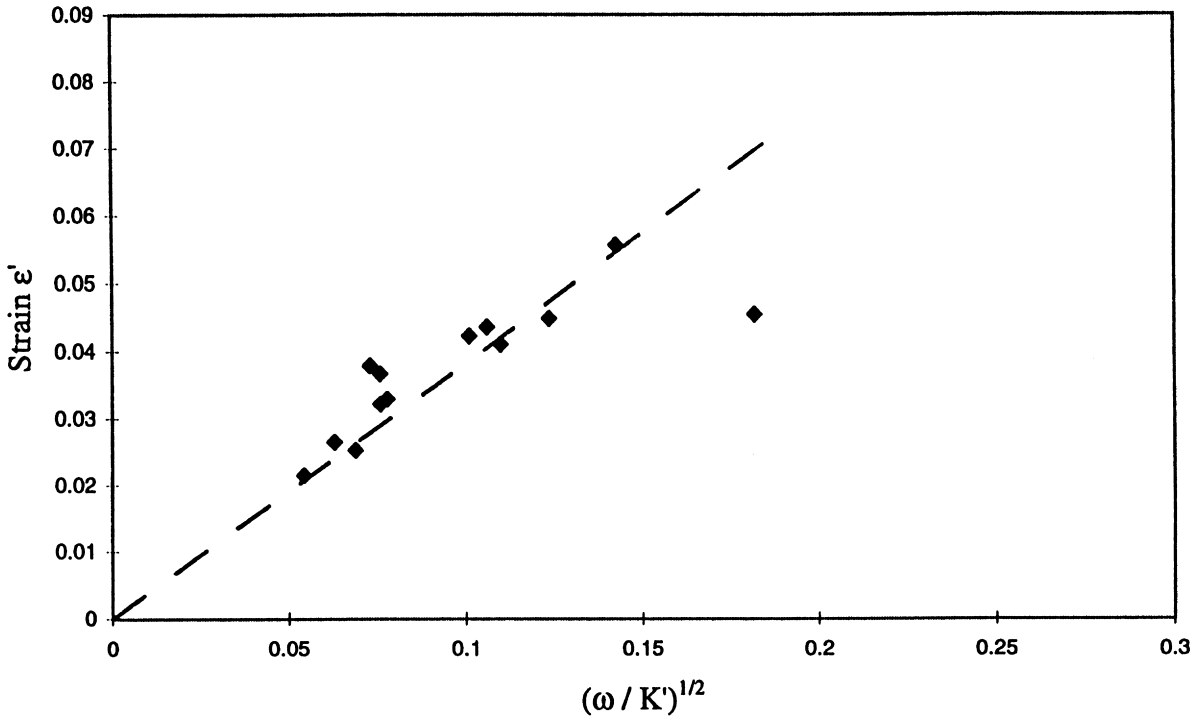

Fig. 7. Strain ε' vs. $(\omega/K')^{1/2}$.

The fracture strain of the equivalent thermodynamically reversible fiber, ε_i, is given by [18]

$$\varepsilon_i = [2\omega W_c/K_i]^{1/2} \tag{2}$$

which is the strain at which the equivalent Hookean fiber of modulus K_i reaches the fracture stress σ_*; i.e. $\varepsilon_i = \sigma_*/K_i$. A plot of ε_i against $(\omega/K_i)^{1/2}$ is of equal favor with that of Fig. 3. Accordingly, with the exception of an obvious low point in Fig. 4, linearity is the case. However, the slope yields a lower value of 0.078 GPa for W_c. As neither analysis is preferable, we average to obtain $W_c = 0.083$ GPa for the most reliable value of the work of rupture of the perfect fiber. If $\sigma_* = 7.5$ GPa for the perfect fiber, then $K_c = 339$ GPa and $\varepsilon_c = 0.022$.

The failure of the two analyses to provide the same result for W_c may not be a fault of the theory but, rather, a fault of the data. If we throw out the low point ($\sigma_* = 0.97$ GPa) the first analysis barely changes to $W_c = 0.089$ GPa but the second rises appreciably to $W_c = 0.085$ GPa, giving an average of $W_c = 0.087$ GPa. If the strength of the perfect fiber is 7.5 GPa, then $K_c = 323$ GPa and $\varepsilon_c = 0.023$. Such values are consistent with Fig. 2.

Determinations of K_i and ε_i require an assessment of the limiting slope of the stress-strain curve as $\sigma, \varepsilon \to 0$; i.e.

$$\lim_{\substack{\sigma\to 0\\ \varepsilon\to 0}} \left(\frac{\sigma}{\varepsilon}\right) = K_i.$$

Of course, this is extremely difficult to accurately determine and involves considerable subjective opinion, as the preceding article suggests [18, Fig. 4]. It might be more reasonable to calculate theoretically both ε_i and K_i. The fusion theory gives ε_i as

$$\varepsilon_i = 0.632\varepsilon_* = \varepsilon' \tag{3}$$

hence

$$K_i = \sigma_*/\varepsilon' = K'. \tag{4}$$

In this article we distinguish these calculated quantities from their experimental analogs with the *prime* superscript. Such calculated values (K', ε') on average differ from the experimental values (K_i, ε_i) by about 4%. A plot of K' against ω is shown in Fig. 5. In this figure we expect K'_c to lie between 275 GPa and perhaps 400 GPa. We can refine this by analyses of Fig. 6 where σ_* vs. $(\omega K')^{1/2}$ and Fig. 7 where ε' vs. $(\omega/K')^{1/2}$. From the respective slopes we find W'_c to be 0.086 and 0.075 GPa, giving an average of $W'_c = 0.081$ GPa for the perfect fiber. Accepting $\sigma_c = 7.5$ GPa as the fiber strength, we must have $K'_c = 347$ GPa and $\varepsilon' = 0.022$.

Again, we drop the low point ($\sigma_* = 0.097$ GPa), to obtain respective values of $W'_c = 0.088$ and 0.084 GPa, for an average of $W'_c = 0.086$ GPa, and $\sigma_c = 7.5$ GPa, $K'_c = 327$ GPa, $\varepsilon' = 0.023$ for the perfect fiber.

Therefore, we conclude from all of the foregoing results that for the perfect fiber: $\sigma_c = 7.5$ GPa; 0.081 GPa $< W_c <$ 0.087 GPa; 323 GPa $< K_c <$ 347 GPa; and $0.022 < \varepsilon_c <$ 0.023.

The subscript "c" here denotes the perfect fiber (crystal) of finite molecular weight polymer.

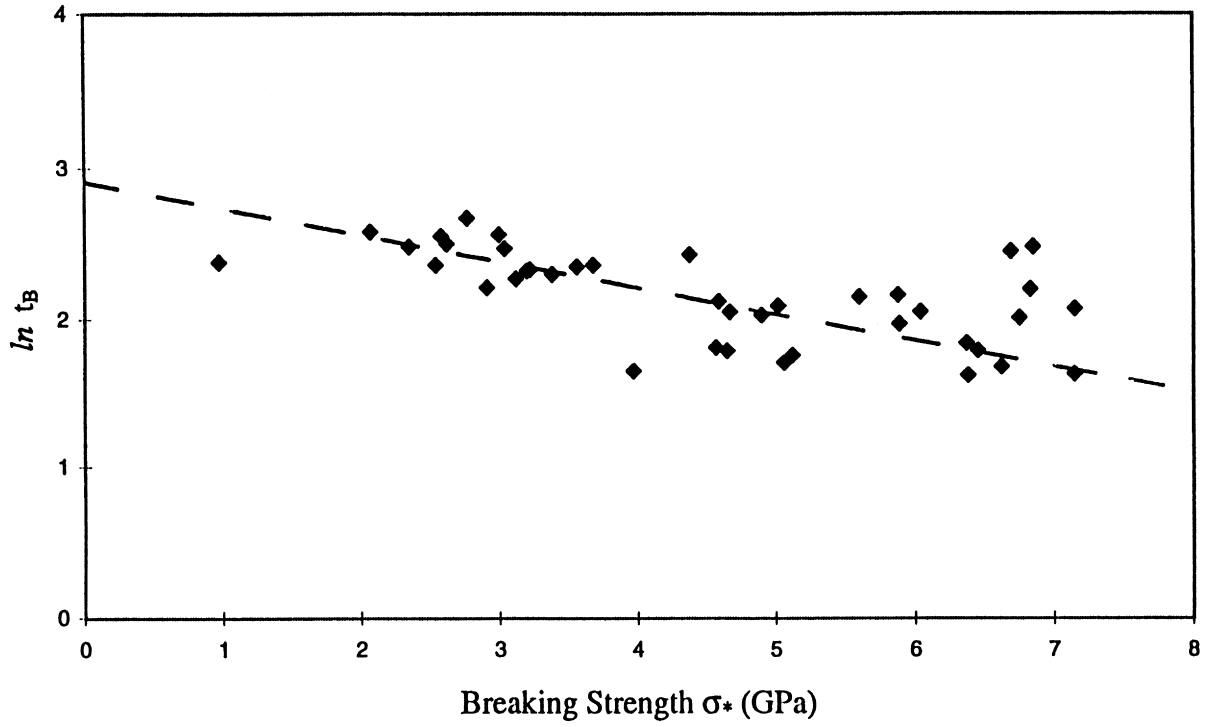

Fig. 8. Linear variation of ln (t_B) with strength.

4. Confirmations of the fusion theory

The fusion theory predicts that σ_* and ε_i are proportional to $(\omega K_i)^{1/2}$ and $(\omega/K_i)^{1/2}$, respectively with an identical proportionality constant of $(2W_c)^{1/2}$. Both variations are in fact linear, at least for $\omega > 0.8$. The theory might be increasingly unreliable as crystallinity decreases further. Whether the low point ($\sigma_* = 0.97$ GPa) is an indication of this or simply a spurious point we cannot say. At large crystallinities, in the "nearly perfect" fiber region, the theory appears quite accurate.

The value of $W_c = 0.084 \pm 0.003$ GPa obtained from the slopes is in good accord with the fusion theory, which gives for polyethylene [27] at 300°K, with $\Delta H_v = 0.293$ GPa [28] and $T_0 = 423$°K, $W_c \approx 0.087$ GPa. Here ΔH_v is the heat of fusion of the perfect fiber (polyethylene crystal), and T_0 is the melting temperature of the unstressed perfect fiber with fixed ends. This calculated result must be high because a variation of ΔH_v with temperature is not taken into account. Over a temperature range of 123°K such a variation should reduce W_c by a small amount since ΔH_v must decrease as temperature decreases. The theoretical and experimental values of W_c therefore appear to be in good agreement.

Is it possible that chain scission can account for our observed results? According to Boudreaux [13], the bond strength of a polyethylene molecule is ~19 GPa, the *c*-axis modulus is ~300 GPa, and the strain at break is ~33%. This strain is 15 times greater than our experimental value of 2.2% for the perfect fiber. Our directly measured breaking strains actually decrease as fiber perfection increases, so it is impossible to understand how a strain of 33% could be obtained for the perfect fiber under any condition. Of greater significance is the measurement of the *maximum* crystalline strain in a polyethylene high-strength fiber at 240°K by Moonen, et al. [29] Maximum crystal strain is identical to the perfect fiber failure strain at 240°K. They reported ε_c (240°K) ≈ 0.024, which by nature of the experiment should be a little low. The fusion theory predicts [27] $\varepsilon_* = \varepsilon_c \approx 0.0265$ at 240°K. However, this value must be a little high because the theoretical calculation assumes a constant heat of fusion. Regardless of the precise value, the two figures are in remarkable agreement, hence the Moonen et al. result assumes substantial importance as independent evidence favoring the fusion theory, particularly since it is *directly* determined by X-ray, free of the problems of mechanical analyses of fibers. Further, our experimental stresses yield ~7.5 GPa for the strength of the perfect fiber, about 2.5 times smaller than Boudreaux's value. The only place of minimal agreement is with the modulus. As Boudreaux's value of strength is the most conservative in the literature for bond scission, we cannot give any credence to such a mechanism of fiber failure.

Linear variation of ln(t_b) with σ_*: According to the result presented in the preceding article [18], the logarithm of the time-to-break in a constant rate of strain deformation is a linear function of the breaking stress. For the 40 results in Tables 2 and 3 the strain rate, $\dot{\varepsilon}$, was 0.00667 s^{-1}, and the time-to-break is $t_b = \varepsilon_*/\dot{\varepsilon}$. From the plot shown in Fig. 8 the

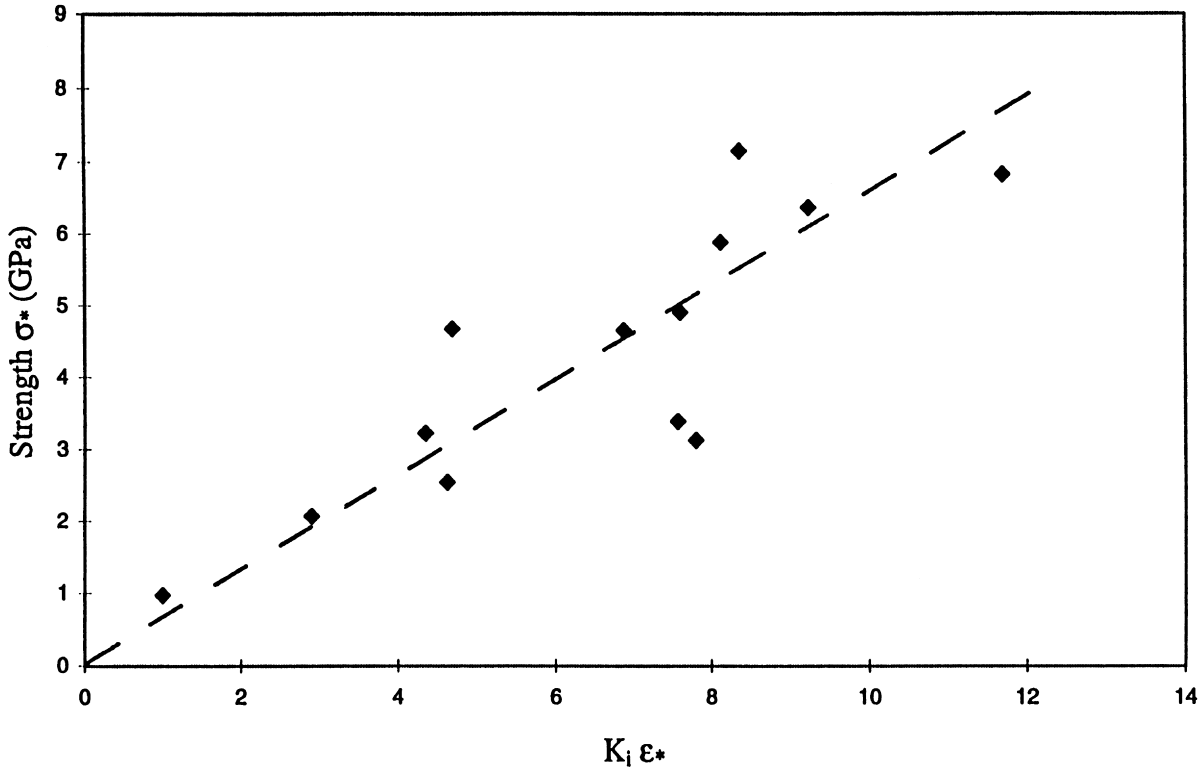

Fig. 9. Linear variation of strength with $K_i\varepsilon_*$; slope = 0.657.

intercept yields an apparent activation energy of 19.37 kcal/mol (81.8 kJ/mol) and the slope gives an apparent activation volume of 4.12×10^{-7} m^3/mol. Both results are in agreement with those obtained [18] from similar literature data [1]. In fact, they are in agreement with predictions in the preceding article [18]. If we have two identical fibers stretched at different rates $\dot{\varepsilon}_1$ and $\dot{\varepsilon}_2$ until they break at stress $\sigma_* = \sigma_1 \equiv \sigma_2$ at respective times τ_1 and τ_2, we must have from our earlier work [18, Eq. (11)]

$$\tau_1\dot{\varepsilon}_1 = \tau_2\dot{\varepsilon}_2. \tag{5}$$

Using the earlier data [18, Fig. 2] for τ_1, $\dot{\varepsilon}_1$, the intercept in Fig. 8 (herein) is calculated with Eq. (5) to be ln (τ_2) = 2.65, and the slopes of the two figures must be similar, and they are. These findings are convincing of the correctness of our treatment of imperfect fibers. This is also additional proof that the Zhurkov equation [14] holds for constant strain rate deformations [18]. However, these numbers are totally inconsistent with bond scission [18].

Linear variation of σ_* with $K_i\varepsilon_*$: In the preceding article [18] it was argued that the breaking time t_b was identical to a particular relaxation (or retardation) time, specifically the one associated with the fracture process. For a constant strain rate deformation this requires that the relationship between breaking stress and strain is [18]

$$\sigma_* = 0.632K_i\varepsilon_*, \tag{6}$$

from which we have the theoretical results ε', K'

$$\varepsilon' = 0.632\varepsilon_*,$$

$$K' = \sigma_*/\varepsilon'.$$

Validation of Eq. (6) constitutes proof that breaking time is identical to a visco-elastic relaxation time, and therefore fiber fracture is a normal visco-elastic response of a fiber to a tensile load. Whatever visco-elastic mechanism allows molecular slip generates fiber failure. As already shown [18], this mechanism is stress-induced melting (for finite molecular weight polymers).

To prove Eq. (6) a plot of the data in Table 3 is shown in Fig. 9. The plot is indeed linear and the slope is 0.657, only a 4% variation from the theory. The result is quite similar to that already given [18]. Of course, some scatter of the data is evident in the figure, but linearity of the behavior is quite convincing the coordinate origin is an indisputable point through which the slope-line must pass.

It is to be pointed out, however, that all data in Tables 2 and 3 plotted in the same manner give a straight line but with a slope of 0.690. Because we believe there is a natural tendency to underestimate K_i, the initial slope of the stress-strain curve, this discrepancy is not particularly disturbing. However, it is recognized that a spectrum of relaxation times may have to be considered if, after very careful determinations of K_i, similar slopes persist in future studies.

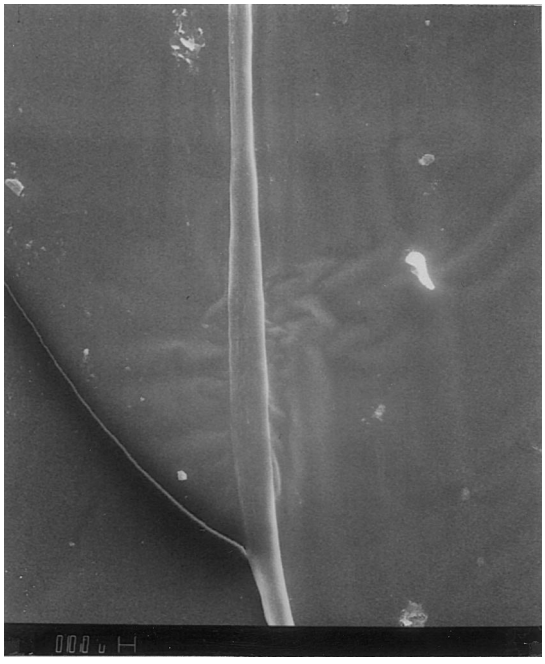

Fig. 10. Non-uniformity of UHMWPE Fiber via SEM.

The modulus of the perfect fiber (crystal). The modulus of the perfect fiber K_c is, in fact, the *c*-axis modulus of the polymer crystal. We found herein for polyethylene

$$K_c = 335 \pm 12 \text{ GPa},$$

which is based on tensile experiments, but not on the homogeneous stress distribution assumption. Our value, though not directly measured, is experimentally determined. It is in good agreement with the theoretical value of 349 GPa recently reported by Meier [30]. Our experimental value is also in close agreement with 340 GPa calculated by Mizushima and Simanouchi [31] over 50 years ago, similarly, with the experimental result of 329 GPa determined by neutron scattering [32], which is of particular interest because both results are free of the homogeneous stress assumption. Concordance between the results of two quite different experimental techniques is encouraging.

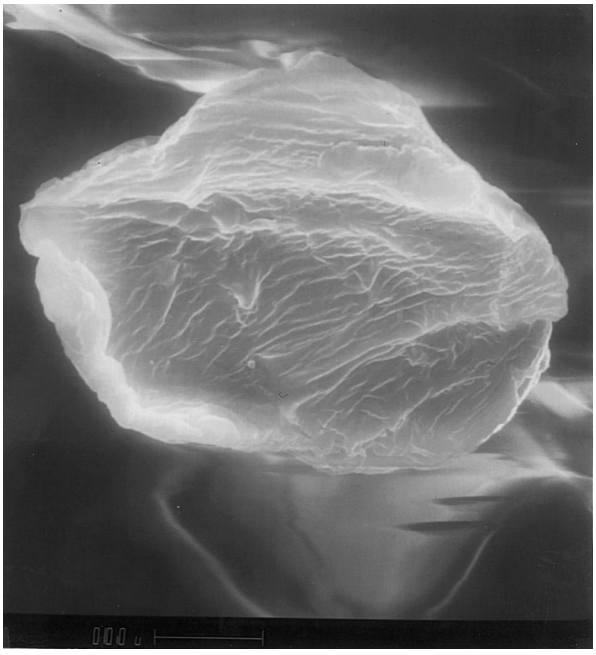

Fig. 11. Cross-section of UHMWPE Fiber.

Table 4
Relative standard deviations for the fibers in Table 3. (Relative standard deviations (in percents) appear in parentheses)

σ_* GPa	RSD (%)	K_i GPa	RSD (%)	ε_*	RSD (%)
0.97	(20)	13.9	(14)	0.072	(28)
2.07	(16)	32.9	(18)	0.088	(22)
2.54	(2.7)	65.1	(14)	0.071	(19)
3.12	(23)	120	(17)	0.065	(20)
3.22	(10)	63	(27)	0.069	(13)
3.38	(17)	113	(12)	0.067	(10)
4.65	(20)	172	(25)	0.040	(20)
4.67	(6.4)	142	(8.7)	0.052	(4.8)
4.90	(17)	149	(15)	0.051	(14)
5.88	(8.5)	140	(7.7)	0.058	(7)
6.37	(8.8)	220	(12)	0.042	(4.8)
6.83	(20)	195	(23)	0.060	(16)
7.15	(39)	246	(11)	0.034	(41)

An important aspect of our result is that it is an indirect average of 13 separate long fibers severed into 58 individual test lengths, i.e. an indirect average of 58 Instron measurements. Erratic, spurious readings, whether low or high, common to such measurements are contributory only in so far as they affect the average. This is the only rational way to obtain meaningful data in this field as a single datum should not be considerable reliable.

4.1. Non-uniformity of fibers

Although a long fiber appears uniform, its cross-section area and shape can vary considerably along its length. We determine the average area of the entire fiber and use that value to compute stresses and moduli of the various test lengths cut from the fiber. Consequently, the apparent stress on a test length of smaller than average area is less than its actual value. The opposite is true for larger than average areas. Therefore, the large variations in strength among the 4 or 5 test lengths of a fiber might signify non-uniformity of cross-section area rather than any number of supposed factors affecting strength. By such reasoning low strength lengths are as likely to be wrong as high strength lengths. It cannot be presumed that low strength results from premature fracture because of flaws or that high strength is more correct because of an absence of flaws. Instead, the only meaningful result is an average over all test lengths from the same long fiber. Such a procedure, though not perfect, must surely provide more reliable results.

Fig. 10 shows a region of a fiber where the diameter of the

thickest section appears to be almost double that of thinnest section. However, we really do not know if the section is circular or flattened. As the average cross-section area of the entire fiber is used to calculate the strength, the thin part of the fiber will yield a lower breaking strength than its true value. The opposite is true for thick sections.

In Fig. 11 the fiber is viewed end on. Clearly, the fiber is not uniformly round. Accordingly, we should be wary about measuring cross-section area with a micrometer. It cannot give correct data about these cross-sections.

Finally, the relative standard deviations, expressed in percentages, of the main fibers in this report—those appearing in Table 3—are listed in Table 4. The variations reflect in large part the cross-sectional deviations of the test lengths from the average cross-section of the parent fiber that is used to compute stresses. The data are indicative primarily of fiber non-uniformity, we believe.

5. Conclusions

This study confirms that fiber failure is a result of stress-induced melting if constituent polymers are of finite molecular weight. No evidence of a bond scission mechanism was observed. In our study of breaking time influenced by stress it was found that, in a constant strain-rate deformation, the apparent activation energy for fiber rupture is 81.81 kJ/mol, which converts into an actual activation energy of 107.7 kJ/mol (25.6 kcal/mol). This value is the heat of fusion of ~31 contiguous methylene units at 25°C, about the activation energy of flow (failure) expected of a fusion mechanism of fracture [18]. The fracture time is a visco-elastic relaxation time characteristic of fiber failure that yields a direct relationship between strength and strain, $\sigma_* = 0.632 K_i \varepsilon_*$, which is verified by our data. For a perfect fiber the relationship reduces to $\sigma_c = K_c \varepsilon_c$. We found $\varepsilon_c \approx 0.0225$, or $\sigma_c \approx 0.0225\ K_c$ for the *macroscopic* perfect polyethylene fiber (a *macroscopic* crystal).

The fusion theory predicts the work of rupture of the equivalent fiber [18] as $W_i < \omega \Delta H_v (1 - T/T_0)$ and a linear relationship between σ_* and $(\omega K_i)^{1/2}$, from which the value of W_c is obtained. Our data verify such a linear relationship with $W_c \approx 0.084$ GPa, cf. the theoretical (fusion) value of 0.087 GPa [27]. Strength of the perfect polyethylene fiber, by slight extrapolation is found to be 7.5 GPa, which in combination with W_c yields a crystal modulus of $K_c \approx 335$ GPa, a value quite close to several literature reports. Each (and all) of these factors is confirmatory of stress-induced fusion as the mechanism of rupture.

To assess fairly the significance of this work, it is necessary to fix in mind a clear picture of the fusion theory as applicable to perfect (ideal) and imperfect (real) polymer fibers. Fusion theory is phenomenological thermodynamics involving only a general system that is characterized by various state variables. Fusion is a change in state from crystal (solid) to melt (liquid). Its transition thermodynamics are universal, independent of specific models. However specific factual details are relevant. For example, is the melt phase a true random state or is some remnant of order retained upon melting a perfect polymer fiber?

Our system is a crystal of individual molecules incapable of supporting an equilibrium load in the melt phase—i.e. a system of finite molecular weight molecules. In four very general easy steps [27] one can obtain the crystal fusion work W_c (which must be reversible work):

$$W_c = \Delta H(1 - T/T_0).$$

The heat of fusion, ΔH, is assumed constant and T_0 is the melting temperature at $W_c = 0$. There are no models here, no wheels, gears, pulleys, gadgets, etc. Nothing whatsoever to dispute. We have only a simple universal system (crystal) having mechanical work done on it (to induce fusion) in accordance with elementary universal phenomenological laws of thermodynamics.

Normally, polymers are not completely crystalline, so we apply the equation to the crystalline phase only, or to an *ideal* comparable macroscopic *perfect* fiber of complete crystallization and orientation, i.e. a perfect macroscopic single polymer crystal, homogeneous and uniform. A tiny assumption is now made: the fiber is Hookean in its elastic response. And that's it! The fiber must melt at its appointed stress σ_c unless another failure mechanism of lower work is available. If not, the fiber (crystal) will cease to be a fiber at its critical load σ_c. It cannot exist as a fiber at a greater load (at constant T, P) unless it can repeal the 1st and 2nd laws of thermodynamics.

With regard to polyethylene, the above fusion equation allows an estimate of the perfect fiber failure work [27]. If $T_0 = 423$°K, $T = 298$°K, and $\Delta H_v = 0.293$ GPa, we have $W_c \approx 0.087$ GPa. There are no flaws, defects, cross-sections, and other hazards to taint the calculation, only pure, simple, elementary, phenomenological thermodynamics [27]. Yet when we compare this to our experimental value of ~0.084 GPa, culled from the experimental slopes of Figs. 3, 4, 6 and 7, the agreement is astonishing, even more so when we realize that the theoretical value must be a little high. A very important implication from this is that our *real* fibers, displayed in the above figures, are apparently devoid of those frequently cited defects and flaws that prevent fibers from reaching their full strength (somewhere between 20 and 100 GPa, according to the scissionists), or that they are less important than previously thought.

Suppose, however, fiber failure really does occur by bond scissions and not by fusion. If the 1st and 2nd laws of thermodynamics are still in force, it is required that scission failure work be less than the fusion work above. Being as generous as possible we assign it the value 0.082 GPa and a fracture stress > 19 GPa so as to include all estimates. The fiber of course remains Hookean in accord with all empirical evidence. Then, its modulus must be $K_c > 2200$ GPa. Another maximum strength sometimes claimed for

polyethylene is 35 GPa. Now, we need a modulus of ~7500 GPa!

Fusion theory [27] is persuasive and compelling. It ties together with a single thread of consistency most if not all empirical observations. Consider the crystal modulus (polyethylene). Most theoretical calculations place it $300 < K_c < 400$ GPa, and our data agree. This gives a strength of $7.1 < \sigma_c < 8.2$ GPa, which is the maximum range consistently observed, notwithstanding sporatic spurious values in excess. We found herein $\sigma_c \approx 7.5$ GPa.

Fusion theory is powerful [27]; it will attract serious consideration and competent analysis. For a perfect fiber it can give the failure work; the deformational changes in fiber energy, enthalpy, entropy, volume, Poisson's ratio, pressure; and the variations of modulus with temperature and with pressure. Not a single adjustable parameter is involved. It is the only theory of strength capable of such quantitative and semi-quantitative predictions.

Acknowledgements

It is with great pleasure that the author (KJS) acknowledges the generous support of this work by the McIntire–Stennis program.

References

[1] Smith P, Lemstra P. J Mater Sci 1980;15:505.
[2] Smith P, Lemstra PJ. Polymer 1980;21:1341.
[3] Smith P, Lemstra PJ, Booij HC. J Polym Sci, Phys Ed 1981;19:877.
[4] Smith P, Lemstra PJ, Pijpers JPL, Kiel AM. Colloid Polym Sci 1981;259:1070.
[5] Smith P, Lemstra PJ. Makromol Chem 1979;180:2983.
[6] Smith P, Lemstra PJ, Kalb B, Pennings AJ. Polym Bull 1979;1:733.
[7] Kalb B, Pennings AJ. J Mater Sci 1980;15:2584.
[8] Kalb B, Pennings AJ. Polymer 1980;21:3.
[9] Smook J, Torfs JCM, van Hutten PE, Pennings AJ. Polym Bull 1980;2:293.
[10] Smook J, Pennings AJ. J Appl Polym Sci 1982;27:2209.
[11] Smook J, Pennings AJ. Polym Bull 1983;9:75.
[12] Smook J, Pennings AJ. Polym Bull 1983;10:291.
[13] Boudreaux DS. J Polym Sci, Phys Ed 1973;11:1285.
[14] Zhurkov S. Int J Fract Mech 1965;1:311.
[15] Zhurkov S, Korskov VE. J Polym Sci, Phys Ed 1974;12:385.
[16] Zhurkov S, Abasov SA. Vysokomol soyedineniya 1962;4:1703.
[17] Zhurkov S, Savostin A Ya, Tomashevsky EE. Dokl Akad Nauk USSR 1964;159:303.
[18] Smith Jr. KJ, Wang J. Polymer 1999;40:7251.
[19] Smith Jr. KJ. Poly Sci Eng 1990;30:437.
[20] Pennings JP, Dijkstra DJ, Pennings AJ. J Mater Sci 1991;26:4721.
[21] Young RJ, Lovell PA. Introduction to polymers, 2nd ed. London: Chapman and Hall, 1991. p. 266.
[22] Alexander LE. X-ray diffraction and methods in polymer science. New York: Wiley-Interscience, 1965.
[23] Prevorsek DC, Mark HF, Bikales NM, Overlerger CG, Menges G. Ultimate properties, uniaxial systems. In: Mark HF, Bikales NM, Overlerger CG, Menges G, editors. Encyclopedia of Polym Sci Eng, 2nd ed. New York: Wiley, 1989. p. 803 Supplement.
[24] Smith P, Lemstra PJ, Pijpers J. J Polym Sci, Phys Ed 1982;20:2229.
[25] Sakurada I, Nukushina Y, Ito T. J Polym Sci 1962;57:651.
[26] Dijkatra DJ, Pennings AJ. Polym Bull 1988;19:481.
[27] Smith Jr. KJ. Compt Theor Polym Sci 1997;7:139.
[28] Quinn FA, Mandelkern L. J Am Chem Soc 1958;80:3178.
[29] Moonen JAHM, Roovers WAC, Meier RJ, Kipp BJ. J Polym Sci, Phy Ed 1992;30:361.
[30] Meier RJ. Macromolecules 1993;26:4376.
[31] Mizushima S, Simanouchi T. J Am Chem Soc 1949;71:1320.
[32] Fanconi B, Rabolt JF. J Polym Sci, Phys Ed 1985;23:1201.